Cite as: D. Wang *et al.*, *Science* 10.1126/science.aao1797 (2018).

Evidence for Majorana bound states in an iron-based superconductor

Dongfei Wang[1,2]*, Lingyuan Kong[1,2]*, Peng Fan[1,2]*, Hui Chen[1], Shiyu Zhu[1,2], Wenyao Liu[1,2], Lu Cao[1,2], Yujie Sun[1,3], Shixuan Du[1,3,4], John Schneeloch[5]†, Ruidan Zhong[5], Genda Gu[5], Liang Fu[6], Hong Ding[1,2,3,4]‡, Hong-Jun Gao[1,2,3,4]‡

[1]Beijing National Laboratory for Condensed Matter Physics and Institute of Physics, Chinese Academy of Sciences, Beijing 100190, China. [2]School of Physical Sciences, University of Chinese Academy of Sciences, Beijing 100190, China. [3]CAS Center for Excellence in Topological Quantum Computation, University of Chinese Academy of Sciences, Beijing 100190, China. [4]Collaborative Innovation Center of Quantum Matter, Beijing 100190, China. [5]Condensed Matter Physics and Materials Science Department, Brookhaven National Laboratory, Upton, NY 11973, USA. [6]Department of Physics, Massachusetts Institute of Technology, Cambridge, MA 02139, USA.

*These authors contributed equally to this work.

†Present address: Physics Department of the University of Virginia, 382 McCormick Rd., Charlottesville, VA 22904-4714, USA.

‡Corresponding author. Email: dingh@iphy.ac.cn, hjgao@iphy.ac.cn

The search for Majorana bound states (MBSs) has been fueled by the prospect of using their non-Abelian statistics for robust quantum computation. Two-dimensional superconducting topological materials have been predicted to host MBSs as zero-energy modes in vortex cores. By using scanning tunneling spectroscopy on the superconducting Dirac surface state of the iron-based superconductor $FeTe_{0.55}Se_{0.45}$, we observe a sharp zero-bias peak inside a vortex core that does not split when moving away from the vortex center. The evolution of the peak under varying magnetic field, temperature, and tunneling barrier is consistent with the tunneling to a nearly pure MBS, separated from non-topological bound states. This observation offers a potential platform for realizing and manipulating MBSs at a relatively high temperature.

Majorana bound states (MBSs) in condensed matter systems have attracted tremendous interest owing to their non-Abelian statistics and potential applications in topological quantum computation (*1*, *2*). A MBS is theoretically predicted to emerge as a spatially localized zero-energy mode in certain *p*-wave topological superconductors in one and two dimensions (*3*, *4*). Although the material realization of such *p*-wave superconductors has remained elusive, other platforms for MBSs have recently been proposed using heterostructures between conventional *s*-wave superconductors and topological insulators (*5*), nanowires (*6*–*8*), quantum anomalous Hall insulator (*9*), or atomic chains (*10*), where the proximity effect on a spin-non-degenerate band creates a superconducting topological state. Various experimental signatures of MBSs (*11*–*14*), or Majorana chiral modes (*15*) have been observed in these heterostructures, but clear detection and manipulation of MBSs are often hindered by the contribution of non-topological bound states and complications of material interface.

Very recently, using high-resolution angle-resolved photoemission spectroscopy (ARPES), a potential platform for MBSs was discovered in the bulk superconductor $FeTe_{0.55}Se_{0.45}$, with a superconducting transition temperature T_c = 14.5 K and a simple crystal structure (Fig. 1A). Because of the topological band inversion between the p_z and d_{xz}/d_{yz} bands around the $\overline{\Gamma}$ point (*16*, *17*) and the multi-band nature (Fig. 1B), this single material naturally has a spin-helical Dirac surface state with an induced full superconducting (SC) gap and a small Fermi energy (Fig. 1C) (*18*); these properties would create favorable conditions for observing a pure MBS (*5*) that is isolated from other non-topological Caroli-de Gennes-Matricon bound states (CBSs) (*19*, *20*). The combination of high-T_c superconductivity and Dirac surface states in a single material removes the challenging interface problems in previous proposals, and offers clear advantages for detecting and manipulating MBSs.

Motivated by the above considerations, we carried out a high-resolution scanning tunneling microscopy/spectroscopy (STM/S) experiment on the surface of $FeTe_{0.55}Se_{0.45}$, which has a good atomic resolution revealing the lattice formed by Te/Se atoms on the surface (Fig. 1D). We start with a relatively low magnetic field of 0.5 T along the *c*-axis at a low temperature of 0.55 K, with a clear observation of vortex cores in Fig. 1E. At the vortex center, we observe a strong zero-bias peak (ZBP) with a full width at half maximum (FWHM) of 0.3 meV and an amplitude of 2 relative to the intensity just outside the gapped region. Outside of the vortex core, we clearly observe a superconducting spectrum with multiple gap features, similar to the ones observed by previous STM studies

on the same material (*21*, *22*). These different SC gaps correspond well with the SC gaps on different Fermi surfaces of this material observed by previous ARPES studies (*23*) [more details in table S1 of (*24*)]. We note a similar ZBP was reported previously (*22*).

We next demonstrate in Fig. 2 and fig. S4 (*24*) that across a large range of magnetic fields the observed ZBP does not split when moving away from a vortex center. It can be clearly seen from Fig. 2, A to D, that the ZBP remains at the zero energy while its intensity fades away when moving away from the vortex center. The non-split ZBP contrasts sharply with the split ZBP originating from CBS observed in conventional superconductors (*19*, *20*), and is consistent with tunneling into an isolated Majorana bound state in a vortex core of a superconducting topological material (*5*, *25*–*27*). We then extract the position-dependent values of the ZBP height and width using simple Gaussian fits of the data in Fig. 2C, and obtain the spatial profile shown in Fig. 2E; the decaying profile has a nearly constant linewidth of about 0.3 meV in the center, which is close to the total width (~ 0.28 meV) contributed from the STM energy resolution [~ 0.23 meV as shown in part I of (*24*)] and the thermal broadening ($3.5k_BT$ @ 0.55 K ~ 0.17 meV). We further compare the observed ZBP height with a theoretical MBS spatial profile obtained by solving the Bogoliubov-de Gennes equation analytically (*5*, *25*) or numerically (*26*, *27*). By using the parameters of E_F = 4.4 meV, Δ_{sc} = 1.8 meV, and $\xi_0 = v_F/\Delta_{sc}$ = 12 nm, which are obtained directly from the topological surface state by our STS and ARPES results (Fig. 2F) (*18*), the theoretical MBS profile matches the experimental one well (Fig. 2G).

The observation of a non-split ZBP, which is different from the split ZBP observed in a vortex of the $Bi_2Te_3/NbSe_2$ heterostructure (*13*, *28*, *29*), indicates that the MBS peak in our system is much less contaminated by non-topological CBS peaks, which is made possible by the large Δ_{sc}/E_F ratio in this system. In a usual topological insulator/superconductor heterostructure, this ratio is tiny, on the order of 10^{-3} – 10^{-2} (*28*). This has been shown to induce, in addition to the MBS at the zero energy, many CBSs, whose level spacing is proportional to Δ_{sc}^2/E_F. As a result, these CBSs are crowded together very close to the zero energy, making a clean detection of MBS from the dI/dV spectra difficult (*29*). However, on the surface of $FeTe_{0.55}Se_{0.45}$, the value of Δ_{sc}^2/E_F is about 0.74 meV, which is sufficiently large to push most CBSs away from the zero energy (*24*), leaving the MBS largely isolated and unspoiled. We note that a large energy separation (0.7 meV) between the ZBP and the CBS was observed in fig. S3, E to H, in agreement with Δ_{sc}^2/E_F of the topological surface states [for details, see part IV of (*24*)]. We also note that all the bulk bands in this multi-band material have fairly small values of E_F thanks to large correlation-induced mass renormalization, ranging from a few to a few tens meV, thus their values of Δ_{sc}^2/E_F are also quite large [> 0.2 meV as shown table S1 of (*24*)]. These large bulk ratios enlarge the energy level spacing of CBSs inside the bulk vortex line, which helps reduce quasiparticle poisoning of the MBS at low temperature [see part II of (*24*) for more details].

It has been predicted (*30*) that the width of the ZBP from tunneling into a single isolated MBS is determined by thermal smearing ($3.5k_BT$), tunneling broadening, and STM instrumentation resolution. We measure the tunneling barrier evolution of the ZBP (Fig. 3A). Robust ZBPs can be observed over two orders of magnitude in tunneling barrier conductance, with the width barely changing (Fig. 3B). We also note the linewidth of ZBPs is almost completely limited by the combined broadening of energy resolution and STM thermal effect, suggesting that the intrinsic width of the MBS is much smaller, and our measurements are within the weak tunneling regime.

However, we do observe some other ZBPs with a larger broadening (Fig. 3C). Interestingly, a larger ZBP broadening is usually accompanied with a softer superconducting gap, or the FWHM of ZBP increases with increasing sub-gap background conductance. The sub-gap background conductance, which is determined by factors such as the strength of scattering from disorder and quasiparticle interactions (*31*–*33*), introduces a gapless fermion bath that can poison the MBS, as explained previously (*34*). The effect of quasiparticle poisoning is to reduce the MBS amplitude and increase its width. This scenario is likely the origin of a larger broadening of ZBP accompanied by a softer gap.

It has been pointed out by previous theoretical studies (*35*–*37*) that the properties of the bulk vortex line, such as its chemical potential, have a significant influence on the Majorana mode on the surface. In order to further characterize the effects of bulk vortex lines, we have monitored the temperature evolution of a ZBP. As shown in Fig. 3D, the ZBP intensity measured at a vortex center decreases with increasing temperature, and becomes extremely weak at 4.2 K and totally invisible at 6.0 K. A peak associated with a CBS would persist to higher temperatures and exhibit simple Fermi-Dirac broadening up to about $T_c/2$ (about 8 K), below which the superconducting gap amplitude is almost constant, as observed in our previous ARPES measurement (*18*). Our observation (Fig. 3D) contradicts this expectation and indicates an additional suppression mechanism that is likely related to the poisoning of MBS by thermally excited quasiparticles. From the extraction of ZBPs amplitude measured on several different vortices (three cases are shown in Fig. 3E), we find that most of the observed ZBPs vanish around 3 K, which is higher than the temperature in many previous Majorana platforms (*11*, *38*). This vanishing temperature is comparable to the energy level spacing of the bulk vortex line as discussed above; thus, the temperature dependence we find is consistent with

a case of a MBS poisoned by thermally induced quasiparticles inside the bulk vortex line [for details see (*24*)].

Our observations provide strong evidence for tunneling to an isolated Majorana bound state; many alternative trivial explanations [part III of (*24*)] cannot account for all the observed features. It is technically possible to move a vortex by a STM tip, which in principle can be used to exchange MBSs inside vortices (Fig. 3F), consequently demonstrating non-Abelian statistics under a sufficiently low ($k_BT << \Delta_{sc}^2/E_F$) temperature (*2*). The high transition temperature and large superconducting gaps in this superconductor offer a promising platform to fabricate robust devices for topological quantum computation.

REFERENCES AND NOTES

1. A. Y. Kitaev, Fault-tolerant quantum computation by anyons. *Ann. Phys.* **303**, 2–30 (2003). doi:10.1016/S0003-4916(02)00018-0
2. C. Nayak, S. H. Simon, A. Stern, M. Freedman, S. Das Sarma, Non-Abelian anyons and topological quantum computation. *Rev. Mod. Phys.* **80**, 1083–1159 (2008). doi:10.1103/RevModPhys.80.1083
3. A. Y. Kitaev, Unpaired Majorana fermions in quantum wires. *Phys. Uspekhi* **44** (10S), 131–136 (2001). doi:10.1070/1063-7869/44/10S/S29
4. N. Read, D. Green, Paired states of fermions in two dimensions with breaking of parity and time-reversal symmetries and the fractional quantum Hall effect. *Phys. Rev. B* **61**, 10267–10297 (2000). doi:10.1103/PhysRevB.61.10267
5. L. Fu, C. L. Kane, Superconducting proximity effect and majorana fermions at the surface of a topological insulator. *Phys. Rev. Lett.* **100**, 096407 (2008). doi:10.1103/PhysRevLett.100.096407 Medline
6. R. M. Lutchyn, J. D. Sau, S. Das Sarma, Majorana fermions and a topological phase transition in semiconductor-superconductor heterostructures. *Phys. Rev. Lett.* **105**, 077001 (2010). doi:10.1103/PhysRevLett.105.077001 Medline
7. Y. Oreg, G. Refael, F. von Oppen, Helical liquids and Majorana bound states in quantum wires. *Phys. Rev. Lett.* **105**, 177002 (2010). doi:10.1103/PhysRevLett.105.177002 Medline
8. A. C. Potter, P. A. Lee, Multichannel generalization of Kitaev's Majorana end states and a practical route to realize them in thin films. *Phys. Rev. Lett.* **105**, 227003 (2010). doi:10.1103/PhysRevLett.105.227003 Medline
9. X.-L. Qi, T. L. Hughes, S.-C. Zhang, Chiral topological superconductor from the quantum Hall state. *Phys. Rev. B* **82**, 184516 (2010). doi:10.1103/PhysRevB.82.184516
10. S. Nadj-Perge, I. K. Drozdov, B. A. Bernevig, A. Yazdani, Proposal for realizing Majorana fermions in chains of magnetic atoms on a superconductor. *Phys. Rev. B* **88**, 020407 (2013). doi:10.1103/PhysRevB.88.020407
11. V. Mourik, K. Zuo, S. M. Frolov, S. R. Plissard, E. P. A. M. Bakkers, L. P. Kouwenhoven, Signatures of Majorana fermions in hybrid superconductor-semiconductor nanowire devices. *Science* **336**, 1003–1007 (2012). doi:10.1126/science.1222360 Medline
12. S. Nadj-Perge, I. K. Drozdov, J. Li, H. Chen, S. Jeon, J. Seo, A. H. MacDonald, B. A. Bernevig, A. Yazdani, Topological matter. Observation of Majorana fermions in ferromagnetic atomic chains on a superconductor. *Science* **346**, 602–607 (2014). doi:10.1126/science.1259327 Medline
13. H.-H. Sun, K.-W. Zhang, L.-H. Hu, C. Li, G.-Y. Wang, H.-Y. Ma, Z.-A. Xu, C.-L. Gao, D.-D. Guan, Y.-Y. Li, C. Liu, D. Qian, Y. Zhou, L. Fu, S.-C. Li, F.-C. Zhang, J.-F. Jia, Majorana Zero Mode Detected with Spin Selective Andreev Reflection in the Vortex of a Topological Superconductor. *Phys. Rev. Lett.* **116**, 257003 (2016). doi:10.1103/PhysRevLett.116.257003 Medline
14. M. T. Deng, S. Vaitiekėnas, E. B. Hansen, J. Danon, M. Leijnse, K. Flensberg, J. Nygård, P. Krogstrup, C. M. Marcus, Majorana bound state in a coupled quantum-dot hybrid-nanowire system. *Science* **354**, 1557–1562 (2016). doi:10.1126/science.aaf3961 Medline
15. Q.-L. He, L. Pan, A. L. Stern, E. C. Burks, X. Che, G. Yin, J. Wang, B. Lian, Q. Zhou, E. S. Choi, K. Murata, X. Kou, Z. Chen, T. Nie, Q. Shao, Y. Fan, S.-C. Zhang, K. Liu, J. Xia, K. L. Wang, Chiral Majorana fermion modes in a quantum anomalous Hall insulator-superconductor structure. *Science* **357**, 294–299 (2017). doi:10.1126/science.aag2792 Medline
16. Z.-J. Wang, P. Zhang, G. Xu, L. K. Zeng, H. Miao, X. Xu, T. Qian, H. Weng, P. Richard, A. V. Fedorov, H. Ding, X. Dai, Z. Fang, Topological nature of the FeSe 0.5 Te 0.5 superconductor. *Phys. Rev. B* **92**, 115119 (2015). doi:10.1103/PhysRevB.92.115119
17. X.-X. Wu, S. Qin, Y. Liang, H. Fan, J. Hu, Topological characters in Fe (Te 1 – x Se x) thin films. *Phys. Rev. B* **93**, 115129 (2016). doi:10.1103/PhysRevB.93.115129
18. P. Zhang, K. Yaji, T. Hashimoto, Y. Ota, T. Kondo, K. Okazaki, Z. Wang, J. Wen, G. D. Gu, H. Ding, S. Shin, Observation of topological superconductivity on the surface of an iron-based superconductor. *Science* **360**, 182–186 (2018). doi:10.1126/science.aan4596 Medline
19. C. Caroli, P. G. de Gennes, J. Matricon, Bound Fermion states on a vortex line in a type II superconductor. *Phys. Lett.* **9**, 307–309 (1964). doi:10.1016/0031-9163(64)90375-0
20. H. F. Hess, R. B. Robinson, J. V. Waszczak, Vortex-core structure observed with a scanning tunneling microscope. *Phys. Rev. Lett.* **64**, 2711–2714 (1990). doi:10.1103/PhysRevLett.64.2711 Medline
21. T. Hanaguri, S. Niitaka, K. Kuroki, H. Takagi, Unconventional s-wave superconductivity in Fe(Se,Te). *Science* **328**, 474–476 (2010). doi:10.1126/science.1187399 Medline
22. F. Massee, P. O. Sprau, Y.-L. Wang, J. C. S. Davis, G. Ghigo, G. D. Gu, W.-K. Kwok, Imaging atomic-scale effects of high-energy ion irradiation on superconductivity and vortex pinning in Fe(Se,Te). *Sci. Adv.* **1**, e1500033 (2015). doi:10.1126/sciadv.1500033 Medline
23. H. Miao, P. Richard, Y. Tanaka, K. Nakayama, T. Qian, K. Umezawa, T. Sato, Y.-M. Xu, Y. B. Shi, N. Xu, X.-P. Wang, P. Zhang, H.-B. Yang, Z.-J. Xu, J. S. Wen, G.-D. Gu, X. Dai, J.-P. Hu, T. Takahashi, H. Ding, Isotropic superconducting gaps with enhanced pairing on electron Fermi surfaces in FeTe 0.55 Se 0.45. *Phys. Rev. B* **85**, 094506 (2012). doi:10.1103/PhysRevB.85.094506
24. Materials and methods are available as supplementary materials.
25. Y. Wang, L. Fu, Topological Phase Transitions in Multicomponent Superconductors. *Phys. Rev. Lett.* **119**, 187003 (2017). doi:10.1103/PhysRevLett.119.187003 Medline
26. C.-K. Chiu, M. J. Gilbert, T. L. Hughes, Vortex lines in topological insulator-superconductor heterostructures. *Phys. Rev. B* **84**, 144507 (2011). doi:10.1103/PhysRevB.84.144507
27. L.-H. Hu, C. Li, D.-H. Xu, Y. Zhou, F.-C. Zhang, Theory of spin-selective Andreev reflection in the vortex core of a topological superconductor. *Phys. Rev. B* **94**, 224501 (2016). doi:10.1103/PhysRevB.94.224501
28. J.-P. Xu, C. Liu, M.-X. Wang, J. Ge, Z.-L. Liu, X. Yang, Y. Chen, Y. Liu, Z.-A. Xu, C.-L. Gao, D. Qian, F.-C. Zhang, J.-F. Jia, Artificial Topological Superconductor by the Proximity Effect. *Phys. Rev. Lett.* **112**, 217001 (2014). doi:10.1103/PhysRevLett.112.217001
29. J.-P. Xu, M.-X. Wang, Z. L. Liu, J.-F. Ge, X. Yang, C. Liu, Z. A. Xu, D. Guan, C. L. Gao, D. Qian, Y. Liu, Q.-H. Wang, F.-C. Zhang, Q.-K. Xue, J.-F. Jia, Experimental detection of a Majorana mode in the core of a magnetic vortex inside a topological insulator-superconductor Bi(2)Te(3)/NbSe(2) heterostructure. *Phys. Rev. Lett.* **114**, 017001 (2015). doi:10.1103/PhysRevLett.114.017001 Medline
30. F. Setiawan, C.-X. Liu, J. D. Sau, S. Das Sarma, Electron temperature and tunnel coupling dependence of zero-bias and almost-zero-bias conductance peaks in Majorana nanowires. *Phys. Rev. B* **96**, 184520 (2017). doi:10.1103/PhysRevB.96.184520
31. S. Das Sarma, A. Nag, J. D. Sau, How to infer non-Abelian statistics and topological visibility from tunneling conductance properties of realistic Majorana nanowires. *Phys. Rev. B* **94**, 035143 (2016). doi:10.1103/PhysRevB.94.035143
32. Y. Yin, M. Zech, T. L. Williams, X. F. Wang, G. Wu, X. H. Chen, J. E. Hoffman, Scanning tunneling spectroscopy and vortex imaging in the iron pnictide superconductor BaFe1.8Co0.2As2. *Phys. Rev. Lett.* **102**, 097002 (2009). doi:10.1103/PhysRevLett.102.097002 Medline
33. C. Renner, A. D. Kent, P. Niedermann, O. Fischer, F. Lévy, Scanning tunneling spectroscopy of a vortex core from the clean to the dirty limit. *Phys. Rev. Lett.* **67**, 1650–1652 (1991). doi:10.1103/PhysRevLett.67.1650 Medline

34. J. R. Colbert, P. A. Lee, Proposal to measure the quasiparticle poisoning time of Majorana bound states. *Phys. Rev. B* **89**, 140505 (2014). doi:10.1103/PhysRevB.89.140505
35. P. Hosur, P. Ghaemi, R. S. K. Mong, A. Vishwanath, Majorana modes at the ends of superconductor vortices in doped topological insulators. *Phys. Rev. Lett.* **107**, 097001 (2011). doi:10.1103/PhysRevLett.107.097001 Medline
36. H.-H. Hung, P. Ghaemi, T. L. Hughes, M. J. Gilbert, Vortex lattices in the superconducting phases of doped topological insulators and heterostructures. *Phys. Rev. B* **87**, 035401 (2013). doi:10.1103/PhysRevB.87.035401
37. G. Xu, B. Lian, P. Tang, X.-L. Qi, S.-C. Zhang, Topological Superconductivity on the Surface of Fe-Based Superconductors. *Phys. Rev. Lett.* **117**, 047001 (2016). doi:10.1103/PhysRevLett.117.047001 Medline
38. F. Nichele, A. C. C. Drachmann, A. M. Whiticar, E. C. T. O'Farrell, H. J. Suominen, A. Fornieri, T. Wang, G. C. Gardner, C. Thomas, A. T. Hatke, P. Krogstrup, M. J. Manfra, K. Flensberg, C. M. Marcus, Scaling of Majorana Zero-Bias Conductance Peaks. *Phys. Rev. Lett.* **119**, 136803 (2017). doi:10.1103/PhysRevLett.119.136803 Medline
39. J. Wen, G. Xu, Z. Xu, Z. W. Lin, Q. Li, W. Ratcliff, G. Gu, J. M. Tranquada, Short-range incommensurate magnetic order near the superconducting phase boundary in $Fe_{1+\delta}Te_{1-x}Se_x$. *Phys. Rev. B* **80**, 104506 (2009). doi:10.1103/PhysRevB.80.104506
40. J.-X. Yin, Z. Wu, J.-H. Wang, Z.-Y. Ye, J. Gong, X.-Y. Hou, L. Shan, A. Li, X.-J. Liang, X.-X. Wu, J. Li, C.-S. Ting, Z.-Q. Wang, J.-P. Hu, P.-H. Hor, H. Ding, S. H. Pan, Observation of a robust zero-energy bound state in iron-based superconductor Fe(Te,Se). *Nat. Phys.* **11**, 543–546 (2015). doi:10.1038/nphys3371
41. Y. J. Song, A. F. Otte, V. Shvarts, Z. Zhao, Y. Kuk, S. R. Blankenship, A. Band, F. M. Hess, J. A. Stroscio, Invited review article: A 10 mK scanning probe microscopy facility. *Rev. Sci. Instrum.* **81**, 121101 (2010). doi:10.1063/1.3520482 Medline
42. Z. P. Yin, K. Haule, G. Kotliar, Spin dynamics and orbital-antiphase pairing symmetry in iron-based superconductors. *Nat. Phys.* **10**, 845–850 (2014). doi:10.1038/nphys3116
43. S. Rinott, K. B. Chashka, A. Ribak, E. D. L. Rienks, A. Taleb-Ibrahimi, P. Le Fevre, F. Bertran, M. Randeria, A. Kanigel, Tuning across the BCS-BEC crossover in the multiband superconductor Fe_{1+y} Se $_x$ Te_{1-x} : An angle-resolved photoemission study. *Sci. Adv.* **3**, e1602372 (2017). doi:10.1126/sciadv.1602372 Medline
44. Y. Lubashevsky, E. Lahoud, K. Chashka, D. Podolsky, A. Kanigel, Shallow pockets and very strong coupling superconductivity in $FeSe_xTe_{1-x}$. *Nat. Phys.* **8**, 309–312 (2012). doi:10.1038/nphys2216
45. K. T. Law, P. A. Lee, T. K. Ng, Majorana fermion induced resonant Andreev reflection. *Phys. Rev. Lett.* **103**, 237001 (2009). doi:10.1103/PhysRevLett.103.237001 Medline
46. S. M. Albrecht, A. P. Higginbotham, M. Madsen, F. Kuemmeth, T. S. Jespersen, J. Nygård, P. Krogstrup, C. M. Marcus, Exponential protection of zero modes in Majorana islands. *Nature* **531**, 206–209 (2016). doi:10.1038/nature17162 Medline
47. H. Zhang, C.-X. Liu, S. Gazibegovic, D. Xu, J. A. Logan, G. Wang, N. van Loo, J. D. S. Bommer, M. W. A. de Moor, D. Car, R. L. M. Op Het Veld, P. J. van Veldhoven, S. Koelling, M. A. Verheijen, M. Pendharkar, D. J. Pennachio, B. Shojaei, J. S. Lee, C. J. Palmstrøm, E. P. A. M. Bakkers, S. D. Sarma, L. P. Kouwenhoven, Quantized Majorana conductance. *Nature* **556**, 74–79 (2018). doi:10.1038/nature26142 Medline
48. B. E. Feldman, M. T. Randeria, J. Li, S. Jeon, Y. Xie, Z. Wang, I. K. Drozdov, B. Andrei Bernevig, A. Yazdani, High-resolution studies of the Majorana atomic chain platform. *Nat. Phys.* **13**, 286–291 (2016). doi:10.1038/nphys3947
49. S. Jeon, Y. Xie, J. Li, Z. Wang, B. A. Bernevig, A. Yazdani, Distinguishing a Majorana zero mode using spin-resolved measurements. *Science* **358**, 772–776 (2017). doi:10.1126/science.aan3670 Medline
50. D. I. Pikulin, J. P. Dahlhaus, M. Wimmer, H. Schomerus, C. W. J. Beenakker, A zero-voltage conductance peak from weak antilocalization in a Majorana nanowire. *New J. Phys.* **14**, 125011 (2012). doi:10.1088/1367-2630/14/12/125011
51. D. Bagrets, A. Altland, Class D spectral peak in Majorana quantum wires. *Phys. Rev. Lett.* **109**, 227005 (2012). doi:10.1103/PhysRevLett.109.227005 Medline
52. P. Magnée, T. M. Klapwijk, Excess conductance of superconductor-semiconductor interfaces due to phase conjugation between electrons and holes. *Phys. Rev. Lett.* **69**, 510–513 (1992). doi:10.1103/PhysRevLett.69.510 Medline
53. E. J. H. Lee, X. Jiang, R. Aguado, G. Katsaros, C. M. Lieber, S. De Franceschi, Zero-bias anomaly in a nanowire quantum dot coupled to superconductors. *Phys. Rev. Lett.* **109**, 186802 (2012). doi:10.1103/PhysRevLett.109.186802 Medline
54. H. O. H. Churchill, V. Fatemi, K. Grove-Rasmussen, M. T. Deng, P. Caroff, H. Q. Xu, C. M. Marcus, Superconductor-nanowire devices from tunneling to the multichannel regime: Zero-bias oscillations and magnetoconductance crossover. *Phys. Rev. B* **87**, 241401 (2013). doi:10.1103/PhysRevB.87.241401
55. M. Ternes, W.-D. Schneider, J.-C. Cuevas, C. P. Lutz, C. F. Hirjibehedin, A. J. Heinrich, Subgap structure in asymmetric superconducting tunnel junctions. *Phys. Rev. B* **74**, 132501 (2006). doi:10.1103/PhysRevB.74.132501
56. N. Levy, T. Zhang, J. Ha, F. Sharifi, A. A. Talin, Y. Kuk, J. A. Stroscio, Experimental evidence for s-wave pairing symmetry in superconducting $Cu_{(x)}Bi_2Se_3$ single crystals using a scanning tunneling microscope. *Phys. Rev. Lett.* **110**, 117001 (2013). doi:10.1103/PhysRevLett.110.117001 Medline
57. F. Gygi, M. Schluter, Electronic tunneling into an isolated vortex in a clean type-II superconductor. *Phys. Rev. B Condens. Matter* **41**, 822–825 (1990). doi:10.1103/PhysRevB.41.822 Medline
58. H. Nishimori, K. Uchiyama, S.-i. Kaneko, A. Tokura, H. Takeya, K. Hirata, N. Nishida, First observation of the fourfold-symmetric and quantum regime vortex core in YNi_2B_2C by scanning tunneling microscopy and spectroscopy. *J. Phys. Soc. Jpn.* **73**, 3247–3250 (2004). doi:10.1143/JPSJ.73.3247
59. J. Liu, F.-C. Zhang, K. T. Law, Majorana fermion induced nonlocal current correlations in spin-orbit coupled superconducting wires. *Phys. Rev. B* **88**, 064509 (2013). doi:10.1103/PhysRevB.88.064509
60. G. E. Blonder, M. Tinkham, T. M. Klapwijk, Transition from metallic to tunneling regimes in superconducting microconstrictions: Excess current, charge imbalance, and supercurrent conversion. *Phys. Rev. B* **25**, 4515–4532 (1982). doi:10.1103/PhysRevB.25.4515
61. L. Y. L. Shen, J. M. Rowell, Zero-Bias Tunneling Anomalies—Temperature, Voltage, and Magnetic Field Dependence. *Phys. Rev.* **165**, 566–577 (1968). doi:10.1103/PhysRev.165.566
62. J. J. Cha, D. Kong, S.-S. Hong, J. G. Analytis, K. Lai, Y. Cui, Weak antilocalization in $Bi_2(Se_{(x)}Te_{(1-x)})_3$ nanoribbons and nanoplates. *Nano Lett.* **12**, 1107–1111 (2012). doi:10.1021/nl300018j Medline
63. V. Crespo, A. Maldonado, J. Galvis, P. Kulkarni, I. Guillamon, J. G. Rodrigo, H. Suderow, S. Vieira, S. Banerjee, P. Rodiere, Scanning microscopies of superconductors at very low temperatures. *Physica C* **479**, 19–23 (2012). doi:10.1016/j.physc.2012.02.014
64. T. Hanaguri, K. Kitagawa, K. Matsubayashi, Y. Mazaki, Y. Uwatoko, H. Takagi, Scanning tunneling microscopy/spectroscopy of vortices in LiFeAs. *Phys. Rev. B* **85**, 214505 (2012). doi:10.1103/PhysRevB.85.214505
65. N. Hayashi, T. Isoshima, M. Ichioka, K. Machida, Low-Lying Quasiparticle Excitations around a Vortex Core in Quantum Limit. *Phys. Rev. Lett.* **80**, 2921–2924 (1998). doi:10.1103/PhysRevLett.80.2921
66. L. Shan, Y.-L. Wang, B. Shen, B. Zeng, Y. Huang, A. Li, D. Wang, H. Yang, C. Ren, Q.-H. Wang, S. H. Pan, H.-H. Wen, Observation of ordered vortices with Andreev bound states in $Ba_{0.6}K_{0.4}Fe_2As_2$. *Nat. Phys.* **7**, 325–331 (2011). doi:10.1038/nphys1908
67. H. Hu, J.-M. Zuo, J. Wen, Z. Xu, Z. Lin, Q. Li, G. Gu, W. K. Park, L. H. Greene, Phase separation in the iron chalcogenide superconductor $Fe_{1+y}Te_xSe_{1-x}$. *New J. Phys.* **13**, 053031 (2011). doi:10.1088/1367-2630/13/5/053031
68. C. Renner, O. Fischer, Vacuum tunneling spectroscopy and asymmetric density of states of $Bi_2Sr_2CaCu_2O_{8+\delta}$. *Phys. Rev. B Condens. Matter* **51**, 9208–9218 (1995). doi:10.1103/PhysRevB.51.9208 Medline
69. K. Flensberg, Tunnelling characteristics of a chain of Majorana bound states. *Phys. Rev. B* **82**, 180516 (2010). doi:10.1103/PhysRevB.82.180516

ACKNOWLEDGMENTS

We thank Qing Huan, Hiroki Isobe, Xiao Lin, Xu Wu, Kai Yang for technical assistance, and Patrick A. Lee, Tai Kai Ng, Shuheng Pan, Gang Xu, Jia-Xin Yin, Fuchun Zhang, Peng Zhang for useful discussions. **Funding:** This work at IOP is supported by grants from the Ministry of Science and Technology of China (2013CBA01600, 2015CB921000, 2015CB921300, 2016YFA0202300), the National Natural Science Foundation of China (11234014, 11574371, 61390501), and the Chinese Academy of Sciences (XDPB08-1, XDB07000000, XDPB0601). L.F. and G.D.G

are supported by US DOE (DE-SC0010526, DE-SC0012704, respectively). J.S. and R.D.Z. are supported by the Center for Emergent Superconductivity, an EFRC funded by the US DOE. **Author contributions:** H.D., H.G., L.K., Y.S., S.D. designed the experiments. D.W., L.K., P.F., H.C., S.Z., W.L., L.C. performed the STM experiments. J.S., R.Z., and G.G. provided the samples. L.F. provided theoretical models and explanations. All the authors participated in analyzing the experimental data, plotting the figures, and writing the manuscript. H.D. and H.G. supervised the project. **Competing interests:** The authors declare that they have no competing interests. **Data and materials availability:** The data presented in this paper can be found in the supplementary materials.

SUPPLEMENTARY MATERIALS

www.sciencemag.org/cgi/content/full/science.aao1797/DC1
Materials and Methods
Supplementary Text
Figs. S1 to S7
Table S1
References (*39*–*69*)
Data File S1

22 June 2017; resubmitted 11 December 2017
Accepted 27 July 2018
Published online 16 August 2018
10.1126/science.aao1797

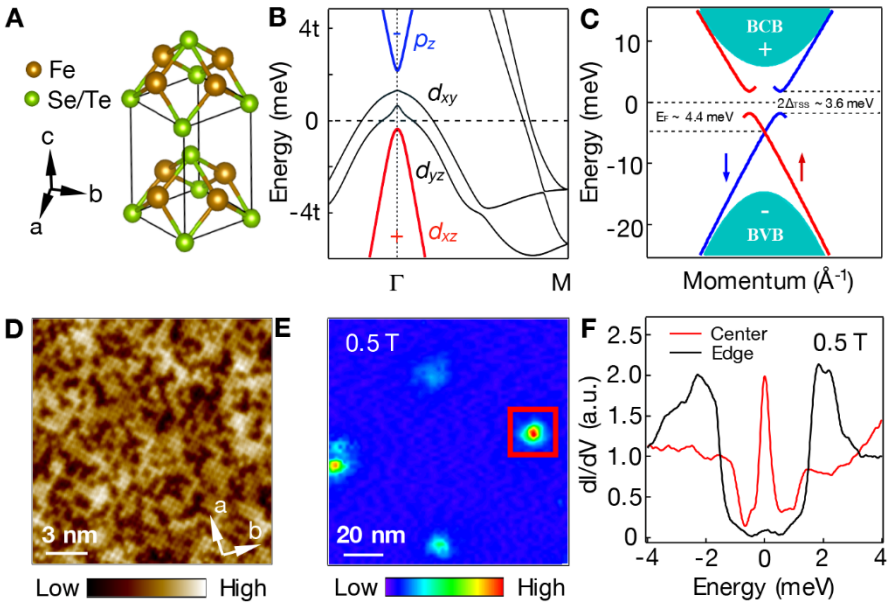

Fig. 1. Band structure and vortex cores of $FeTe_{0.55}Se_{0.45}$. (**A**) Crystal structure of $FeTe_{0.55}Se_{0.45}$. Axis a or b indicates one of Fe-Fe bond directions. (**B**) A first principle calculation of the band structure along the Γ-M direction, adopted from Fig. 1C of (*18*). In the calculations, t = 100 meV, whereas t ~ 12 to 25 meV from ARPES experiments, largely depending on the bands (*23*). (**C**) Summary of superconducting topological surface states on this material observed by ARPES from Ref. (*18*). (**D**) STM topography of $FeTe_{0.55}Se_{0.45}$ (scanning area: 17 nm × 17 nm). (**E**) Normalized zero-bias conductance (ZBC) map measured at a magnetic field of 0.5 T, with the area 120 nm × 120 nm. (**F**) A sharp ZBP in a *dI/dV* spectrum measured at the vortex core center indicated in the red box on (E). Settings: sample bias, V_s = –5 mV; tunneling current, I_t = 200 pA; and temperature, T = 0.55 K.

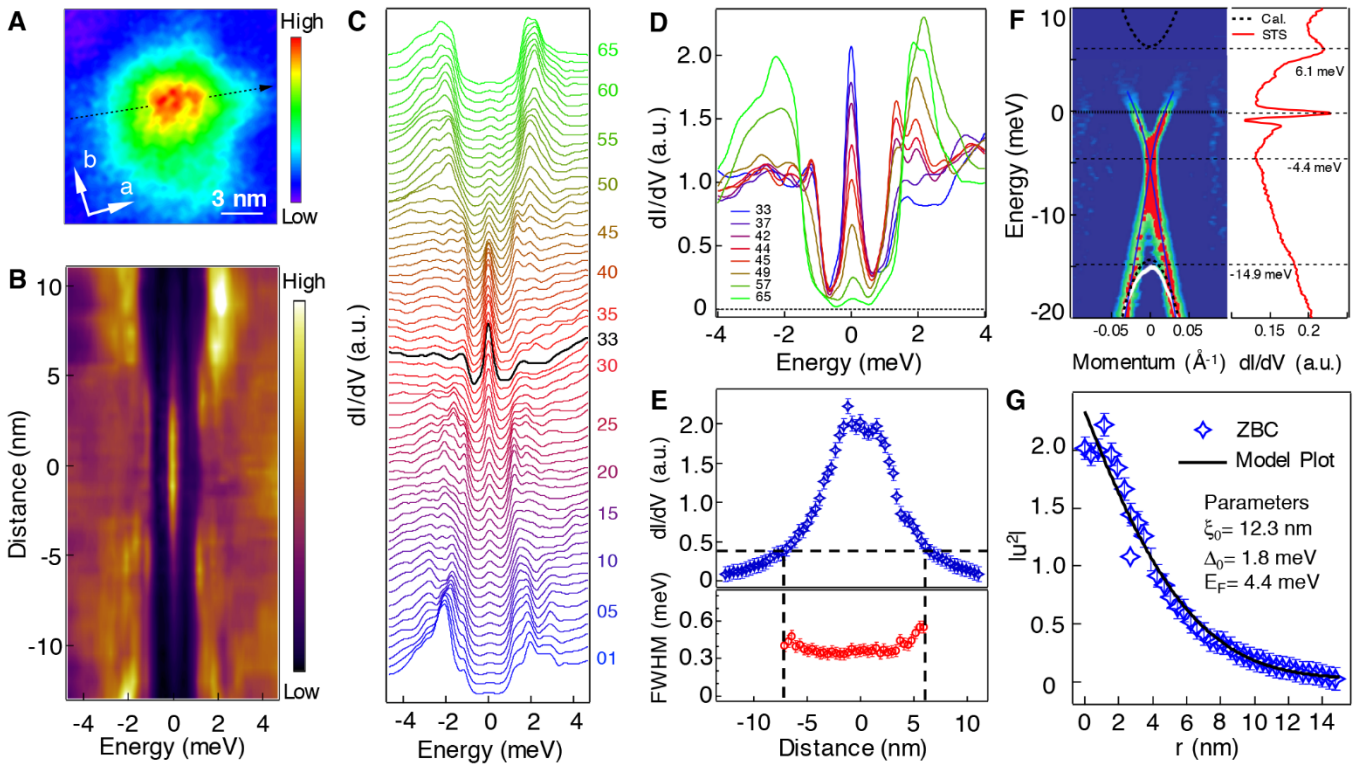

Fig. 2. Energetic and spatial profile of ZBPs. (**A**) A ZBC map (area = 15 nm × 15 nm) around vortex cores. (**B**) A line-cut intensity plot along the black dash line indicated in (A). (**C**) A waterfall-like plot of (B) with 65 spectra, with the black curve corresponding to the one in the core center. (**D**) An overlapping display of 8 *dI/dV* spectra selected from (C). (**E**) Spatial dependence of the height (upper panel) and FWHM (lower panel) of the ZBP (see text). (**F**) Comparison between ARPES and STS results. Left panel: ARPES results on the topological surface states adopted from Ref. (*18*). Black dashed curves are extracted from a first-principle calculation (*37*), with the calculated data rescaled to match the energy positions of the Dirac point and the top of the bulk valence band (BVB). Right panel: a *dI/dV* spectrum measured from -20 meV to 10 meV. (**G**) Comparison between the measured ZBP peak intensity with a theoretical calculation of MBS spatial profile [Part VIII of (*24*)]. The data in (B) to (G) are normalized by the integrated area of each *dI/dV* spectrum. Settings: V_s = –5 mV, I_t = 200 pA, and T = 0.55 K, $B_\perp$ = 0.5 T.

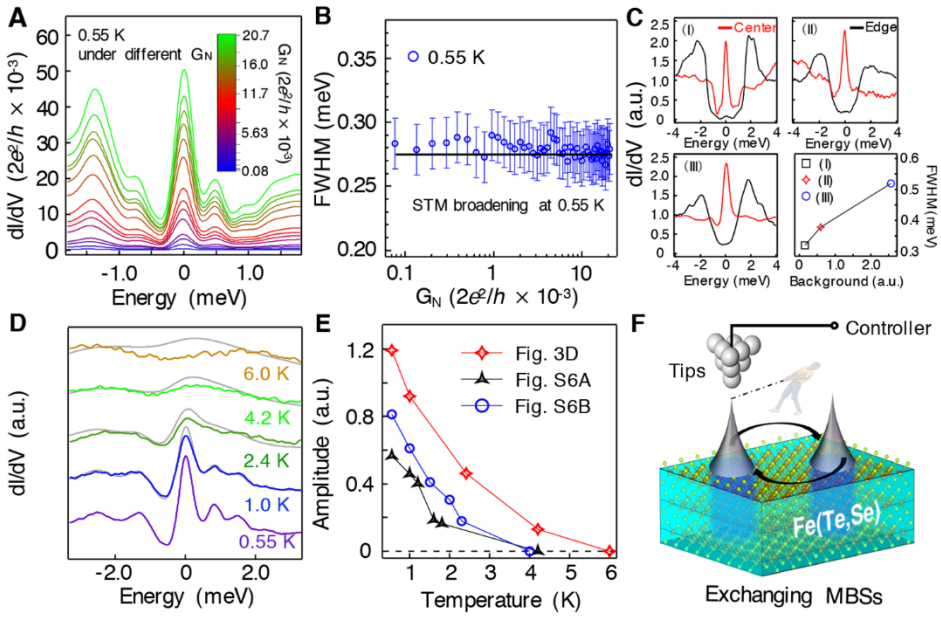

Fig. 3. Temperature and tunneling barrier evolution of ZBPs. (**A**) Evolution of ZBPs with tunneling barrier measured at 0.55 K. $G_N \equiv I_t/V_s$, which corresponds to the energy-averaged conductance of normal states, and represents the conductance of the tunneling barrier. I_t and V_s are the STS setpoint parameters. (**B**) FWHM of ZBPs at 0.55 K under different tunneling barriers. The black solid line is the combined effect of energy resolution [0.23 meV (*24*)] and tip thermal broadening (3.5 k_BT) at 0.55 K. (**C**) FWHM of ZBP at the center of vortex core is larger when the superconducting gap around the vortex core is softer. Background is defined as an integrated area from -1 meV to +1 meV of the spectra at the core edge. (**D**) Temperature evolution of ZBPs in a vortex core. The gray curves are numerically broadened 0.55 K data at each temperature. (**E**) Amplitude of the ZBPs shown in (D) and fig. S6 (*24*) under different temperatures. The amplitude is defined as the peak-valley difference of the ZBP. (**F**) Schematic of a possible way for realizing non-Abelian statistics in a ultra-low-temperature STM experiment which may have an ability to exchange MBSs on the surface of Fe(Te, Se). Settings: (A) and (B) show the absolute value of conductance; $B_\perp = 2.5$ T. In (D) and (E), the data are normalized by integrated area; $V_s = -10$ mV, $I_t = 100$ pA, $T = 0.55$ K, $B_\perp = 4$ T.

Evidence for Majorana bound states in an iron-based superconductor

Dongfei Wang, Lingyuan Kong, Peng Fan, Hui Chen, Shiyu Zhu, Wenyao Liu, Lu Cao, Yujie Sun, Shixuan Du, John Schneeloch, Ruidan Zhong, Genda Gu, Liang Fu, Hong Ding and Hong-Jun Gao

published online August 16, 2018